SIMULATION-BASED OPTIMISATION OF URBAN TRAFFIC FLOW USING MULTI-CRITERIA AND FORECASTING MODELS

Nguyen Quoc Tuan[1,*], Giap Van Quy[1]

DOI: https://doi.org/10.57001/huih5804.2026.123

ABSTRACT

Urban traffic congestion adversely affects operational efficiency, safety and environmental sustainability in developing cities. This study presents an integrated framework combining microscopic traffic simulation (SUMO), multi-criteria decision-making (TOPSIS and PSI) and short-term traffic demand forecasting (ARIMA) to optimise traffic flow along the urban corridor between Hanoi University of Industry (HaUI) and Hanoi National University. Empirical traffic data were collected through on-site surveys and camera-based monitoring, calibrated against a SUMO simulation model and subsequently used to rank two traffic management alternatives. The results demonstrate that signal phase reconfiguration with dedicated turn lanes (Option 2) reduces average vehicle waiting time by approximately 2.71% and increases average travel speed by 3.11% relative to the current state. PSI-based multi-criteria ranking confirms Option 2 as the optimal strategy. ARIMA (2,1,1) forecasting further reveals an estimated reserve operational capacity of approximately 407% between current demand and the infrastructure saturation threshold, indicating that poor signal control rather than physical infrastructure capacity is the primary bottleneck.

Keywords: *Traffic congestion, traffic flow optimisation, SUMO simulation, TOPSIS, PSI, ARIMA, urban mobility, decision support.*

[1]Faculty of Industrial Systems, School of Mechanical and Automotive Engineering, Hanoi University of Industry (HaUI), Vietnam

[*]Email: tuannq@haui.edu.vn

Received: 12/3/2026

Revised: 08/5/2026

Accepted: 25/5/2026

1. INTRODUCTION

Research on urban traffic flow has addressed a broad range of issues related to the understanding, modelling, and optimisation of transportation systems. Early studies primarily focused on establishing theoretical foundations and mathematical formulations to describe traffic dynamics under varying operating conditions, thereby providing the basis for congestion analysis and traffic signal optimisation strategies [1, 4, 11, 16]. Macroscopic, microscopic, and hybrid traffic flow models have been developed to represent different levels of traffic dynamics [4], while fluid-based conceptualisations of traffic streams have contributed to explaining congestion propagation and traffic phase transition phenomena [16]. Despite their theoretical contributions, these studies are generally characterised by a strong emphasis on analytical modelling, with limited integration of real-world traffic data and practical traffic management applications, a limitation that motivates the empirical orientation of more recent investigations.

In parallel with theoretical developments, numerous empirical and simulation–based studies have examined urban traffic corridors, intersections, and freeway systems under diverse operating conditions [2, 6, 7, 10, 14, 15, 17, 18]. Empirical investigations have analysed traffic disturbance factors in Malaysia [2], urban road networks in China [10], transportation systems in developing South Asian cities [14], unsignalised intersections in the Taxila region [15], and selected freeway corridors [6, 18]. Continuous flow analyses on urban expressways have further clarified the relationship between hourly traffic volume and travel time under varying demand conditions [7]. Microscopic simulation platforms, particularly Simulation of Urban MObility (SUMO), have enabled controlled and repeatable evaluation of traffic management strategies, thereby supporting data-driven decision-making [3, 17, 18]. The reliability of simulation-based findings depends critically on systematic model calibration and validation, commonly assessed through the GEH statistic, Root Mean Square Error (RMSE) and Mean Absolute Percentage Error (MAPE) against field-measured volumes [23, 24]. Queueing theory has also been applied to analyse vehicle accumulation and service rate relationships at signalised intersections [20]. Beyond operational efficiency, traffic flow conditions have been

associated with safety risks in confined infrastructure such as tunnels [5] and with vehicle emission patterns affecting environmental sustainability [13]. Although these studies collectively advance empirical understanding, they remain predominantly confined to isolated, case–specific analyses without integrating multi criteria evaluation or demand forecasting within a unified analytical framework.

A particularly important challenge in developing countries is the prevalence of mixed-traffic conditions involving motorcycles, passenger cars, buses, and non-motorised vehicles, which substantially increases the complexity of traffic flow modelling and congestion forecasting [12]. Existing studies consistently demonstrate that local traffic composition, infrastructure constraints, and heterogeneous travel demand characteristics strongly influence congestion formation and operational performance. This structural complexity renders direct application of models developed for homogeneous traffic environments less reliable and underscores the need for context-specific analytical frameworks tailored to mixed-flow urban corridors.

In recent years, multi-criteria decision-making methods and traffic demand forecasting approaches have attracted increasing research attention as complementary tools for traffic management evaluation [9, 22]. Methods such as TOPSIS and PSI have demonstrated potential for ranking traffic intervention scenarios based on multiple performance indicators, while time series forecasting models have been applied to project short-term travel demand under varying growth conditions [9, 22]. Nevertheless, these approaches are typically developed in isolation, forecasting models are rarely integrated with microscopic simulation outputs, and decision-making evaluations seldom incorporate forward-looking demand projections. This disconnect limits the capacity of existing frameworks to assess the long-term robustness of proposed traffic management interventions.

Despite substantial progress across these research directions, existing studies on urban traffic optimisation have predominantly focused on one of three independent approaches:

(i) standalone microscopic traffic simulation [3, 17, 18];

(ii) multi-criteria decision-making methods [8, 19];

(iii) short-term traffic demand forecasting [9, 22]. Limited attention has been given to integrating these approaches within a unified corridor-level analytical framework validated using real-world traffic data. This research gap is particularly acute in developing countries, where urban traffic systems are simultaneously characterised by mixed traffic flows, heterogeneous vehicle compositions, non-uniform infrastructure, and rapidly growing travel demand, conditions that render piecemeal analytical approaches insufficient for informing effective traffic management policy.

To address this gap, the present study selects the Route 32 corridor connecting Hanoi University of Industry and Vietnam National University, Hanoi as a representative case study area. Field surveys (detailed in Section 2.2) reveal severe peak-hour congestion at the Phu Dien Junction, Tran Vy Intersection, and Mai Dich Overpass, attributable to spontaneous parking activities, uncoordinated signal timing, and weak lane discipline compliance. Periodic traffic surges from educational institutions further intensify demand variability, making this corridor a representative case for investigating congestion management in rapidly urbanising developing cities.

Accordingly, this study proposes a four-stage integrated analytical framework combining Simulation of Urban MObility, TOPSIS, PSI, and ARIMA, validated using field-collected traffic data. The framework integrates microscopic traffic simulation with both subjective and objective multi-criteria evaluation mechanisms: TOPSIS is employed to capture residents' perceptions of traffic conditions, while PSI is applied to rank intervention scenarios based on simulation-derived performance indicators. This dual evaluation approach ensures consistency between user-oriented assessments and quantitative operational outcomes. The integration of the ARIMA forecasting model further enables verification of the robustness of the optimal scenarios under projected future demand conditions, thereby extending the analytical scope beyond static scenarios comparison. On this basis, the study develops an evidence-based framework to evaluate existing traffic conditions, rank alternative traffic management scenarios, and assess the reserve capacity of the recommended intervention under anticipated demand growth.

2. METHODOLOGY

2.1. Research framework

The methodology comprises four integrated stages; Stage 1 provides foundational inputs to Stages 2, 3, and 4

in parallel, while Stages 2-4 each build on these shared inputs through distinct analytical pathways to ensure analytical consistency throughout the proposed framework:

First, the field data collected in Stage 1, including traffic density, signal phase duration, and traffic violation frequency, were used both to calibrate the SUMO simulation model in Stage 3 and to construct the input time series for the ARIMA forecasting model in Stage 4. In addition, the Likert-scale survey conducted in Stage 1 provided the basis for determining the relative importance of evaluation criteria through the TOPSIS analysis in Stage 2;

Second, the criterion weights derived from the TOPSIS procedure were integrated into the multi-criteria evaluation framework used to assess the proposed intervention scenarios;

Third, the ten performance indicators generated from the SUMO simulations in Stage 3 were employed as quantitative inputs for the PSI method, enabling objective ranking and comparison of the proposed traffic management scenarios;

Finally, the ARIMA forecasting model developed in Stage 4 utilized the saturation threshold associated with the optimal scenario identified in Stage 3 to quantify the remaining reserve capacity under projected traffic demand conditions. Overall, the proposed analytical workflow helped reduce subjective bias and improve methodological consistency across the different stages of the study.

Stage 1 - Field Data collection: On–site surveys and camera monitoring at peak-hour intersections to collect vehicle density, queue length, cycle time, and traffic disruption data [3, 21].

Stage 2 - Multi-Criteria Evaluation (TOPSIS): Ranking of surveyed user groups by perceived traffic performance using the TOPSIS algorithm (Eq. 1-5), with criterion weights determined by the Point Allocation Method [8].

Stage 3 - Microscopic Simulation (SUMO): Calibrated simulation of the corridor under the current state and two proposed alternatives, generating performance indicators for PSI based optimality ranking (Eq. 6-8) [17, 18].

Stage 4 - Demand Forecasting (ARIMA): Short-term traffic demand forecast using the ARIMA (2,1,1) model (Eq. 12) to validate infrastructure reserve capacity against projected demand growth [22].

2.2. Study corridor and Signal characteristics

Route 32 records approximately 339,500 vehicles per day, with a heterogeneous mix dominated by motorcycles (61%) and passenger cars (25%). Seven signalised intersections regulate flow along the corridor; their timing parameters are summarised in Table 1.

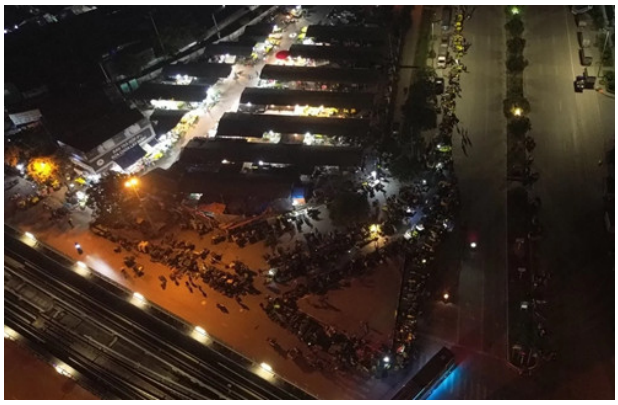

Figure 1. Flower market activity along 70A Street near Route 32 causing roadway obstruction during pre-dawn hours

Table 1. Signalised intersections and traffic signal timing along Route 32

No.	Intersection	Green (s)	Red (s)	Notes
1	Nhon (Route 32 - Tran Huu Duc)	45 - 70	80 - 90	Standard cycle; adjustable based on real-time flow
2	Cau Dien - Nguyen Dong Chi	45 - 70	80 - 90	Standard cycle; adjustable based on real-time flow
3	Cau Dien - Pham Van Dong	45 - 70	80 - 90	Green-phase extended to improve 8-lane throughput
4	Ho Tung Mau - Tran Vy - Le Duc Tho	-	-	Right-turn on-demand; two signal phases deactivated
5	Ho Tung Mau - Nguyen Co Thach	45 - 70	80 - 90	Standard cycle; adjustable based on real-time flow
6	Mai Dich (Ho Tung Mau - Xuan Thuy - Ring Road 3 - Pham Hung)	45 - 70	80 - 90	Roundabout integrated with traffic signals
7	Xuan Thuy - Nguyen Phong Sac - Cau Giay	45 - 70	80 - 90	Sidewalk narrowed to accommodate right-turn lane

Note: Green/red times shown are programmable ranges. Actual values vary according to sensor-detected peak-hour demand. Intersection 4 operates in a free-flow right-turn mode with central signal phases currently suspended.

2.3. Analytical methods and Formulae

2.3.1. TOPSIS method

The TOPSIS (Technique for Order Preference by Similarity to Ideal Solution) method evaluates each alternative by measuring its geometric distance from both the ideal (best) and negative-ideal (worst) solutions across all weighted criteria. Five sequential steps are applied; each step produces intermediate values that feed directly into the next, culminating in the preference index Pi used to populate Table 4 and Table 5.

Step 1: Vector normalisation of the decision matrix

Raw Likert-scale scores from Table 3 contain no unit heterogeneity, but vector normalisation is applied to project all values onto a common unit-hypersphere, eliminating scale dependence before weighting:

$$r_{ij} = \frac{x_{ij}}{\sqrt{\sum_{j=1}^{m} x_{ij}^2}} \quad (1)$$

where x_{ij} is the raw score of criterion *j* for group *i*, r_{ij} is the normalised value and m = 4 is the number of surveyed groups. Squaring and summing within each column ensures the column-norm equals unity, preserving the relative ordering of alternatives.

Step 2: Weighted normalised matrix

Each normalised value r_{ij} is scaled by the criterion weight w_j determined in Table 2 via the Point Allocation Method:

$$v_{ij} = r_{ij}.w_j \quad (2)$$

The resulting matrix v_{ij} reflects both the relative performance of each group and the relative importance of each criterion. Criteria with higher w_j (e.g., Congestion: 0.30) exert proportionally greater influence on the final ranking than lower-weight criteria (e.g., Red Light Wait: 0.15).

Step 3: Ideal and negative-ideal solutions.

For each criterion *j*, the ideal solution A^+ selects the maximum v_{ij} (for benefit criteria) or minimum v_{ij} (for cost criteria) and vice versa for the negative-ideal A^-. This study treats all five criteria as benefit indicators (higher score = better perceived condition), so:

$A^+ = \{\max(v_{ij}) \mid j = 1, \ldots, 5\}$; $A^- = \{\min(v_{ij}) \mid j = 1, \ldots, 5\}$

Step 4: Euclidean separation distances

The Euclidean distance of each alternative from A^+ and A^- is:

$$S_i^+ = \sqrt{\sum_{j=1}^{n}(v_{ij} - A_j^+)^2} \quad (3)$$

$$S_i^- = \sqrt{\sum_{j=1}^{n}(v_{ij} - A_j^-)^2} \quad (4)$$

Si^+ measures proximity to the ideal; Si^- measures proximity to the worst case. Both values appear as columns in Table 4 and Table 5, enabling direct verification of the ranking logic.

Step 5: Relative closeness coefficient

$$P_i = \frac{S_i^-}{S_i^- + S_i^+} \quad (5)$$

$P_i \in [0, 1]$; $P_i = 1$ implies the alternative coincides with the ideal solution, while $P_i = 0$ implies it coincides with the negative-ideal. The P_i values in Table 4 are computed by substituting Si^+ and Si^- from Eq. 3 and 4 into Eq. 5.

2.3.2. PSI method

The Preference Selection Index (PSI) method is applied after simulation to rank traffic alternatives objectively without requiring subjective weight assignment. Each criterion is normalised relative to its reference value (maximum for benefit indicators, minimum for cost indicators), yielding partial preference indices that are summed to produce a total PSI score.

For benefit (maximised) indicators:

$$P_{ij} = \frac{X_{ij}}{max(X_j)} \quad (6)$$

For cost (minimised) indicators:

$$P_{ij} = \frac{min(X_j)}{X_{ij}} \quad (7)$$

Total PSI score for alternative i:

$$S_i = \sum_j P_{ij} \quad (8)$$

where X_{ij} is the simulated value of indicator j for alternative i and X_j, ref is the reference value for indicator j. $P_{ij} \in [0, 1]$; when X_{ij} equals its reference value (X_j, ref), $P_{ij} = 1$, representing perfect alignment for that indicator. When all n = 10 indicators contribute equally, each $P_{ij} = 1/n$. Summing P_{ij} across all n = 10 indicators via Eq. 8 gives the total PSI score reported in Table 12. The alternative with the highest total score is optimal.

2.3.3. SUMO model calibration and Validation metrics

Prior to comparative scenario evaluation, the SUMO simulation model was calibrated and statistically validated using a 21-day field-measured peak-hour traffic volume dataset collected along the Route 32 corridor. The calibration process involved iterative adjustment of key driver-behaviour parameters, including desired speed distribution, minimum gap acceptance, and acceleration/deceleration profiles, until the simulated

traffic volumes at the primary camera measurement location achieved satisfactory agreement with the observed field data. To quantitatively evaluate model validity and calibration fidelity, three complementary statistical indicators were employed: the GEH statistic, Root Mean Square Error (RMSE), and Mean Absolute Percentage Error (MAPE) [23, 24].

(i) GEH statistic

The GEH statistic is a dimensionless index that combines absolute and relative differences, specifically designed for traffic volume validation:

$$GEH = \sqrt{\frac{2(V_{sim} - V_{obs})^2}{V_{sim} + V_{obs}}} \quad (9)$$

where:

V_{sim} = simulated traffic volume at the measurement point (vehicles/hour);

V_{obs} = field-observed traffic volume at the same measurement point (vehicles/hour).

Acceptance criteria are commonly defined as follows: GEH < 5.0 indicates good model fit; GEH ∈ [5.0, 10.0) is considered acceptable; and GEH ≥ 10.0 requires model recalibration [23,24]. The GEH statistic provides a balanced validation measure by combining both absolute and relative error sensitivity across varying traffic volume conditions.

(ii) Root Mean Square Error (RMSE)

RMSE quantifies the average magnitude of absolute deviation between simulated and observed volumes across all n observation periods:

$$RMSE = \sqrt{\frac{1}{n}\sum_{i=1}^{n}(V_{sim,i} - V_{obs,i})^2} \quad (10)$$

where:

n = total number of observation days (n = 21 in this study);

$V_{sim,i}$ = simulated volume on day i (vehicles/hour);

$V_{obs,i}$ = field-observed volume on day i (vehicles/hour);

i = index of the observation day (i = 1, 2,…, 21).

RMSE is expressed in the same unit as the observations (vehicles/hour) and is particularly sensitive to large individual deviations, making it a useful complement to percentage-based metrics.

(iii) Mean Absolute Percentage Error (MAPE)

MAPE expresses the average relative deviation as a percentage of the observed value, providing a scale-independent measure of model accuracy:

$$MAPE = \frac{1}{n}\sum_{i=1}^{n}\frac{|V_{obs,i} - V_{sim,i}|}{V_{obs,i}} \, x \, 100\% \quad (11)$$

where all symbols retain the definitions given above for Eq. 10.

Acceptance criteria: MAPE < 10% is considered acceptable for microsimulation validation; MAPE < 5% indicates high accuracy [23, 24]. The calibration statistics obtained using Eq. 9-11 are presented and discussed in Section 3.1.5 (Tables 8 and 9).

2.3.4. ARIMA forecasting model

The Autoregressive Integrated Moving Average (ARIMA) model captures temporal autocorrelation in the traffic count time series and projects demand over a 10-day forecast horizon. The general ARIMA (p, d, q) equation is:

$$Y_t = c + \sum_{i=1}^{P}\phi_i Y_{t-i} + \varepsilon t + \sum_{j=1}^{q}\theta_j \varepsilon_{t-j} \quad (12)$$

where $\hat{y}_t$ is the predicted vehicle count at time t; $\varphi_1, \ldots, \varphi_p$ are autoregressive coefficients capturing dependence on p previous observations; ε_t is a white noise error term; $\theta_1, \ldots, \theta_q$ are moving average coefficients applied to q previous error terms; and d is the degree of differencing applied to achieve stationarity of the series.

Model parameters were calibrated as ARIMA (2,1,1), $p = 2$, $d = 1$, $q = 1$ based on inspection of the Autocorrelation Function (ACF) and Partial Autocorrelation Function (PACF) of the 21-day vehicle count series. The fitted model is subsequently used to generate the 10-day forecast shown in Figure 7 and to compute the reserve capacity discussed in Section 3.2.4.

According to George Box and Gwilym Jenkins [22], low order ARIMA models ($p + q \leq 3$) can be reliably estimated using approximately 15 - 20 observations after differencing, particularly for time series exhibiting low variability, as reflected by the coefficient of variation observed in this study (CV ≈ 3.1%). After applying first-order differencing ($d = 1$), the time series retained 20 observations, while the autocorrelation function (ACF) and partial autocorrelation function (PACF) patterns indicated cutoffs at $q = 1$ and $p = 2$, respectively, thereby supporting the selection of the ARIMA (2,1,1) structure.

Within the scope of this study, the objective of the model was not to generate long-term trend forecasts, but rather to:

(i) verify the short-term stability of travel demand;

(ii) compare the forecast demand against the saturation threshold of the optimal intervention scenario

to quantify the remaining reserve capacity margin and assess infrastructure robustness under projected demand growth. For these purposes, the ARIMA (2,1,1) model developed from n = 21 observations provides a preliminary yet appropriate statistical basis for short-term forecasting within the scope of this study. The selected forecasting horizon of 10 days corresponds to approximately 48% of the training series length, remaining within commonly accepted practical recommendations for short-term time series forecasting.

3. RESULTS AND DISCUSSION

3.1. Results

3.1.1. Criterion weighting using the point allocation method

Because the influence of evaluation criteria on urban traffic operational performance may vary depending on local traffic characteristics, the determination of criterion weights should incorporate both technical perspectives and the practical mobility demands of road users. Therefore, the research team conducted a survey involving seven (7) participants including three individuals with experience in urban traffic signal system design, two researchers specializing in traffic engineering, and two personnel responsible for traffic corridor management along the Route 32 corridor. Participants were selected based on: (i) knowledge of urban traffic signal systems in Hanoi; (ii) familiarity with mixed-traffic conditions dominated by motorcycles; and (iii) at least five years of professional or research experience related to the study corridor.

Each participant was asked to allocate a total of 100 points across the five evaluation criteria, including congestion, safety, red-light waiting time, sidewalk quality, and parking availability, to reflect the relative priority of each criterion with respect to urban mobility demands within the study area. The average scores obtained for each criterion were subsequently linearly normalized to derive normalized weights with a unit sum, denoted as w_j, which were then used as inputs to Eq. (2) in the TOPSIS method.

Furthermore, to verify the reliability and consistency of the weighting process, the coefficient of variation (CV) was employed to evaluate the level of agreement among the survey participants' scoring results. The results indicated that the CV values for all five criteria were below 20%, demonstrating an acceptable level of reliability and consistency in the weighting process. The final criterion weights are presented in Table 2.

Table 2. Criteria weights determined by the point allocation method (w_j values used in Eq. 2)

Criterion	Congestion	Safety	Red-light waiting time	Sidewalk quality	Parking avail.
Avg. Score (pts)	30	20	15	20	15
Weight w_j (→ Eq. 2)	**0.30**	**0.20**	**0.15**	**0.20**	**0.15**

3.1.2. Multi-Criteria analysis using TOPSIS

Likert-scale survey responses from four resident groups (A-D) at distinct corridor locations constitute the raw decision matrix (Table 3). These values are first normalised via Eq. 1, then weighted by w_j (Eq. 2) and finally processed through Eq. 3-5 to generate the preference indices Pi reported in Tables 4 and 5.

Table 3. Initial decision matrix X (raw Likert scores; input to Eq. 1)

Group	Congestion (w_j= 0.30)	Safety (w_j= 0.20)	Red light wait (0.15)	Sidewalk quality (0.20)	Parking avail. (0.15)
A (Mai Dich)	3	4	2	3	4
B (Le Duc Tho -HoTungMau)	5	3	4	2	3
C (HaUI Entrance)	2	5	1	4	5
D (Thanh Do Supermarket)	4	2	3	5	2

Table 4. TOPSIS ranking results

Group	Si^+ (Eq. 3) → dist. to ideal	Si^- (Eq. 4) → dist. to neg.-ideal	Pi (Eq. 5) = $Si^-/(Si^+ + Si^-)$	Rank	Location
A	0.014	0.011	0.44	3	Mai Dich overpass
B	0.022	0.016	0.42	4	Le Duc Tho - Ho Tung Mau
C	0.015	0.023	0.61	1	HaUI Entrance
D	0.018	0.016	0.47	2	Thanh Do Supermarket

Table 5. Full TOPSIS weighted normalised matrix v_{ij} (Eq. 2)

Grp	Cong.	Safety	RLW	Sidew.	Park.	Si^+	Si^-	Pi	Rank
A	0.0165	0.0148	0.0100	0.0110	0.0111	0.014	0.011	0.44	3
B	0.0279	0.0110	0.0200	0.0076	0.0080	0.022	0.016	0.42	4
C	0.0114	0.0186	0.0050	0.0148	0.0140	0.015	0.023	0.61	1
D	0.0222	0.0076	0.0150	0.0186	0.0060	0.018	0.016	0.47	2

3.1.3. Field data collection, cleaning and statistical analysis

Traffic counts and traffic disturbance events were extracted from roadside cameras over 21 consecutive days (1-21 March 2025) at a fixed 90-second signal cycle. Three sessions recorded missing values ("F") due to camera obstruction. These were imputed using linear interpolation in Python (Pandas interpolate), producing the cleaned dataset in Table 7 that serves as input to the ARIMA model (Eq. 12).

Table 6. Raw camera extracted traffic data

Date	Session	Vehicle count	Cycle time (s)	Disturbance events
01-03-2025	1	640	90	126
02-03-2025	2	617	90	110
03-03-2025	3	654	90	138
04-03-2025	4	F	90	127
05-03-2025	5	622	90	151
06-03-2025	6	635	90	F
07-03-2025	7	629	90	125
08-03-2025	8	648	90	129
09-03-2025	9	**F**	90	131
10-03-2025	10	645	90	115
11-03-2025	11	617	90	121
12-03-2025	12	610	90	118
13-03-2025	13	628	90	114
14-03-2025	14	675	90	115
15-03-2025	15	685	90	112
16-03-2025	16	642	90	116
17-03-2025	17	622	90	118
18-03-2025	18	605	90	114
19-03-2025	19	631	90	113
20-03-2025	20	637	90	110
21-03-2025	21	605	90	111

Note: "F" = missing data due to camera occlusion or sensor failure. Bold "F" cells are highlighted for clarity. Traffic disturbances are defined as vehicle stoppage events in which vehicles were unable to maintain pace with the surrounding traffic stream.

Table 7. Cleaned traffic data after linear interpolation of missing values

Date	Session	Vehicle Count	Cycle Time (s)	Disturbance events
01-03-2025	1	640	90	126
02-03-2025	2	617	90	110
03-03-2025	3	654	90	138
04-03-2025	4	**634***	90	127
05-03-2025	5	622	90	151
06-03-2025	6	635	90	**121***
07-03-2025	7	629	90	125
08-03-2025	8	648	90	129
09-03-2025	9	**634**	90	131
10-03-2025	10	645	90	115
11-03-2025	11	617	90	121
12-03-2025	12	610	90	118
13-03-2025	13	628	90	114
14-03-2025	14	675	90	115
15-03-2025	15	685	90	112
16-03-2025	16	642	90	116
17-03-2025	17	622	90	118
18-03-2025	18	605	90	114
19-03-2025	19	631	90	113
20-03-2025	20	637	90	110
21-03-2025	21	605	90	111

Note: Interpolated values. Linear interpolation formula: $\hat{X}_t = (X_{t-1} + X_{t+1})/2$. Interpolated values represent ≈ 14.3% of observations (3/21 sessions); their influence on series statistics is limited given the low variance of the overall series (CV ≈ 3.1%).

The impact of linear interpolation was evaluated by comparing the ARIMA (2,1,1) model using two datasets:

(i) the complete dataset consisting of 21 observations, including interpolated values;

(ii) a reduced dataset containing 18 actual observations after excluding three occluded days.

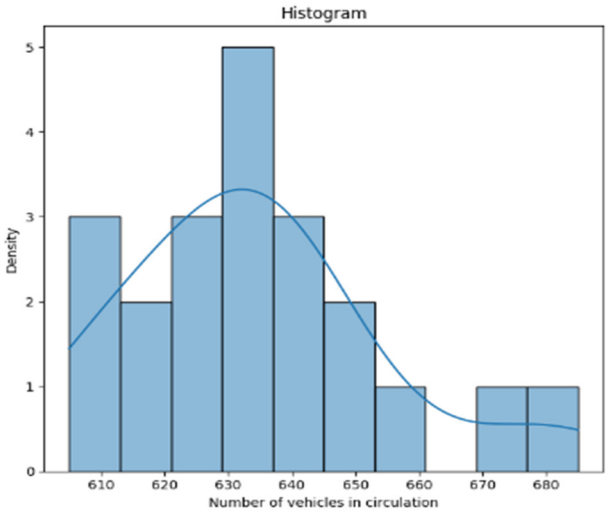

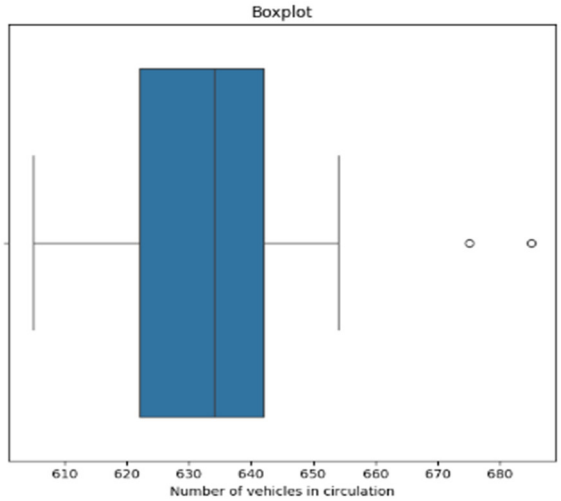

Figure 2. Distribution of daily vehicle counts: histogram (left) and boxplot (right)

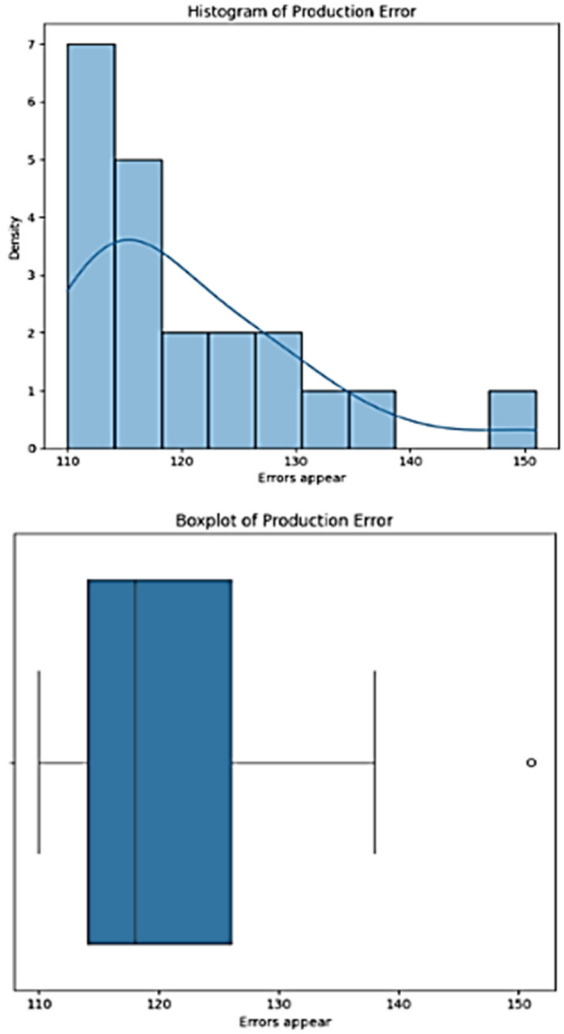

Figure 3. Distribution of daily traffic disturbance counts: histogram and boxplot

The results showed that the RMSE deviation between the two models was less than 1.5 vehicles per hour, while the difference in the 10-day forecast remained below 2%. These findings indicate that the three interpolated values, accounting for 14.3% of the total observations, did not significantly influence the modeling results, which is consistent with the low coefficient of variation of the original time series (CV ≈ 3.1%). Furthermore, the ADF test performed after first-order differencing yielded a *p-value* of 0.018 < 0.05, confirming the stationarity of the time series, which is a necessary condition for ARIMA modelling.

3.1.4. Proposed traffic management alternatives

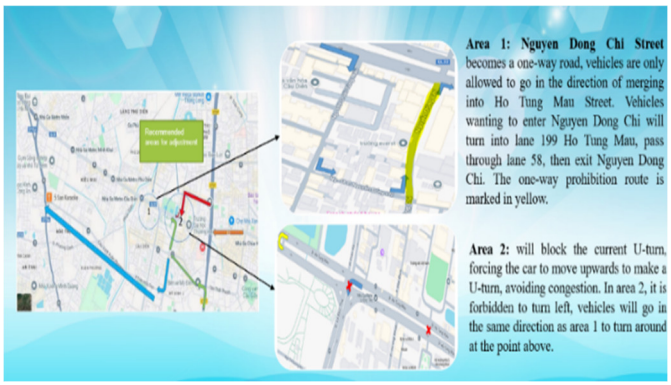

Figure 4. Study corridor from Hanoi National University to HaUI (Source: Google Maps)

Option 1 - Traffic reorganisation with left-turn restrictions: Establishment of one-way schemes in complex zones (Doan Ke Thien - Tran Vy; Nguyen Dong Chi corridor); prohibition of left turns at high-conflict nodes (Route 32-Le Duc Tho); regulated flow at Mai Dich junction and the Pham Hung-Route 32 overpass.

Option 2 - Signal phase reconfiguration with dedicated turn lanes: Separate signal arrows for each movement direction (left, straight, right) at Cau Dien - Nguyen Dong Chi, Ho Tung Mau - Tran Vy and Mai Dich - Xuan Thuy. Total cycle: 75s, allocated proportionally 62% straight, 23% right-turn, 15% left-turn based on observed turning-movement counts.

3.1.5. SUMO Model Calibration and Validation

Following the calibration procedure described in Section 2.3.3, model validity is assessed by comparing simulated peak-hour traffic volumes with the 21-day field-observed dataset at the primary camera measurement point on Route 32. Table 8 presents the day-by-day comparison of observed and simulated volumes, together with the corresponding GEH, MAPE and assessment outcomes for each observation day. Table 9 summarises the aggregate calibration statistics across all 21 days.

Table 8. SUMO model calibration results-observed versus simulated peak-hour traffic volumes at the primary measurement point (Route 32, 1-21 March 2025)

Day	Observed (veh/hr)	Simulated (veh/hr)	Diff (veh/hr)	GEH	MAPE (%)
1	630	647	+17	0.67	2.70
2	625	625	0	0.00	0.00
3*	635	639	+4	0.16	0.63
4	640	647	+7	0.28	1.09
5	618	615	-3	0.12	0.49
6	632	636	+4	0.16	0.63
7	628	632	+4	0.16	0.64
8	641	631	-10	0.40	1.56
9	624	636	+12	0.48	1.92
10*	634	643	+9	0.36	1.42
11	637	636	-1	0.04	0.16
12	643	645	+2	0.08	0.31
13	629	637	+8	0.32	1.27
14	675	677	+2	0.08	0.30
15	685	687	+2	0.08	0.29
16	648	640	-8	0.32	1.23
17*	635	643	+8	0.32	1.26
18	621	626	+5	0.20	0.81
19	633	639	+6	0.24	0.95
20	616	607	-9	0.36	1.46
21	638	655	+17	0.67	2.66
Overall	**637**	**640**	**+4**	**0.26**	**1.04**

Note: Denotes linearly interpolated values (Days 3, 10 and 17) where camera data were unavailable, as described in Table 7. Acceptance criteria: GEH < 5.0 and MAPE < 10% per Dowling et al. [23] and UK Highways Agency [24]. Assessment: Good = GEH < 2.0; Accept = GEH 2.0-5.0; Fail = GEH ≥ 5.0.

Table 9. Aggregate SUMO model calibration statistics (n = 21 observation days)

Metric	RMSE (veh/hr)	MAPE (%)	GEH (mean)	GEH (max)	R^2
Calibration result	8.0	1.04%	0.26	0.67	0.83
Acceptance threshold	-	< 10%	-	< 5.0	-
Assessment	**-**	✓	**-**	✓	**-**

Note: RMSE and MAPE computed over all 21 observation days using Eq. 10 and Eq. 11 respectively. R^2 calculated between the observed and simulated daily volume series. Reference thresholds from Dowling et al. [23] and UK Highways Agency [24].

All 21 GEH values were below 1.0 (mean = 0.26; maximum = 0.67), substantially within the GEH < 5.0 acceptance threshold. The overall MAPE of 1.04% and RMSE of 8.0 vehicles/hour confirm satisfactory agreement between simulated and field-observed volumes at the primary measurement location. The R^2 of 0.83 indicates that the model reproduces approximately 83% of the observed day-to-day demand variability, with residual variance attributable to the stochastic nature of SUMO's driver behaviour module. These outcomes satisfy the validation criteria of Dowling et al. [23] and the UK Highways Agency [24] and confirm that the calibrated model provides a reliable basis for the comparative scenario evaluation reported in Section 3.1.6.

3.1.6. SUMO simulation results and performance comparison

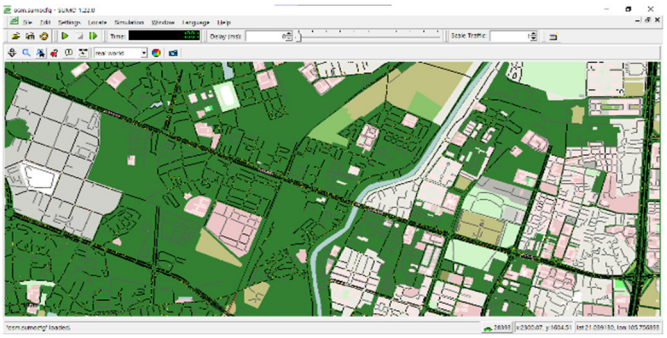

a) Option 1 (left-turn restriction scenario)

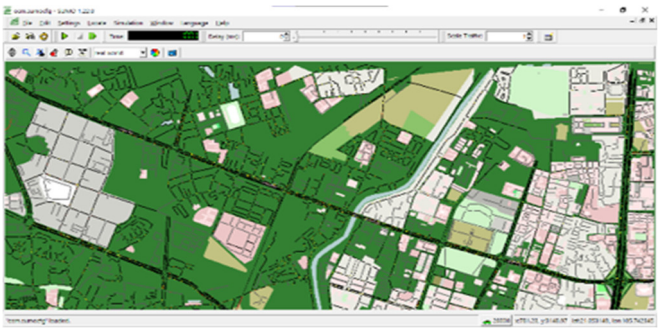

b) Option 2 (signal phase reconfiguration)

Figure 5. SUMO simulation output

Table 10. SUMO simulation performance summary current state vs. Option 1 vs. Option 2 (indicators in bold rows are inputs to PSI decision matrix, Table 11)

Performance indicator	Current state	Option 1	Option 2
Vehicles inserted [→ PSI Table 11]	33,228	33,175	33,152
Vehicles running [→ PSI Table 11]	28,616	28,393	28,338
Vehicles waiting [→ PSI Table 11]	11,760	11,813	11,836
Total irregular movements [→ PSI Table 11]	2,103	1,869	2,005

- Congestion-related	1,002	902	973
- Yielding behaviour	1,065	945	1,018
- Wrong-lane movements	36	21	13
Collisions	0	1	1
Emergency stops	0	5	0
Emergency braking events	2	6	1
Completed trips [→ PSI Table 11]	4,612	4,782	4,814
Avg. distance travelled - km/vehicle [→ PSI Table 11]	1.175	1.184	1.219
Avg. speed - km/h [→ PSI Table 11]	28.908	29.376	29.808
Avg. travel time - s/vehicle [→ PSI Table 11]	210.43	209.87	209.49
Avg. waiting time - s/vehicle [→ PSI Table 11]	102.80	101.81	100.09
Total waiting time - all vehicles, s [→ PSI Table 11]	15,416	18,855	15,858

Note: The bold rows represent the ten performance indicators directly used as inputs for the PSI matrix (Table 11). The non-bold rows are presented solely for reference and comparison purposes and were not included in the PSI scoring process. The throughput indicator (traffic demand input) remained nearly unchanged across all scenarios (approximately 33,152 - 33,228 vehicles), confirming that the observed performance differences were attributable to operational changes rather than variations in traffic demand.

Figure 6. Comparative visualisation of key performance indicators across three simulation scenarios

Note: Comparative performance of the evaluated traffic-management scenarios across the selected PSI indicators. Orange = Current State; Green = Option 1; Purple = Option 2. The vertical axis represents the raw values of each performance indicator. According to the PSI evaluation framework (Tables 11–12), indicators with optimisation direction ↑ MAX include Vehicles inserted, Vehicles running, Completed trips, and Average speed, whereas indicators with optimisation direction ↓ MIN include Vehicles waiting, Irregular movements, Average distance, Average travel time, Average waiting time, and Total waiting time. Emergency stops and Collisions were excluded from the PSI evaluation and are therefore not presented as ranking indicators in this figure.

3.1.7. PSI-based optimality ranking of alternatives

Following simulation, the 10 bold-row indicators from Table 10 were assembled into the PSI decision matrix (Table 11). Each indicator was normalised using Eq. 6 (for benefit/Max criteria) or Eq. 7 (for cost/Min criteria) relative to its reference value, producing partial preference indices P_{ij}. These were summed via Eq. 8 to yield the total PSI score and ranking presented in Table 12.

Table 11. PSI decision matrix-normalised indicator values with criterion direction

Indicator	Current State	Option 1	Option 2	Ref. Value	Eq.
Vehicles inserted	33,228	33,175	33,152	33,228 (Max)	Eq. 6
Vehicles running	28,616	28,393	28,338	28,616 (Max)	Eq. 6
Vehicles waiting	11,760	11,813	11,836	11,760 (Min)	Eq. 7
Irregular movements	2,103	1,869	2,005	1,869 (Min)	Eq. 7
Completed trips	4,612	4,782	4,814	4,814 (Max)	Eq. 6
Avg. distance (km/veh)	1.175	1.184	1.219	1.175 (Min)	Eq. 7
Avg. speed (km/h)	28.909	29.376	29.808	29.808 (Max)	Eq. 6
Avg. travel time (s/veh)	210.43	209.87	209.49	209.49 (Min)	Eq. 7
Avg. waiting time (s/veh)	102.80	101.81	100.09	100.09 (Min)	Eq. 7
Total waiting time (s)	15,416	18,855	15,858	15,416 (Min)	Eq. 7

Note: Indicators associated with operational efficiency and traffic throughput were treated as benefit criteria and normalised using Eq. 6, whereas indicators associated with congestion, delays, and traffic disturbances were treated as cost criteria and normalised using Eq. 7. Reference values correspond to the optimal benchmark value among the evaluated alternatives for each indicator. Traffic volumes were evaluated under mixed-traffic conditions using operationally equivalent traffic-flow measures derived from the SUMO simulation environment.

Table 12. PSI normalised partial scores P_{ij} and total PSI score

Indicator	Current State P_{ij}	Option 1 P_{ij}	Option 2 P_{ij}
Vehicles inserted	0.1001	0.0999	0.0998
Vehicles running	0.1002	0.0995	0.0993
Vehicles waiting	0.1002	0.0998	0.0996

Irregular movements	0.0885	0.0996	0.0928
Completed trips	0.0959	0.0995	0.1001
Avg. distance travelled	0.1002	0.0994	0.0966
Avg. speed	0.0971	0.0987	0.1002
Avg. travel time	0.0998	0.1001	0.1002
Avg. waiting time	0.0975	0.0985	0.1002
Total waiting time	0.0984	0.0804	0.0956
Total PSI Score (Eq. 8)	**0.8783**	**0.9750**	**0.9848**
Ranking	**3rd**	**2nd**	**1st-Optimal**

Note: P_{ij} values represent the normalised partial preference scores obtained from the PSI method for each traffic-performance indicator. Higher P_{ij} values indicate better relative operational performance under the corresponding criterion. The total PSI score was calculated using Eq. 8 as the aggregate preference index across all evaluated indicators. Although certain individual indicators favoured specific alternatives, the final ranking reflects the overall multi-criteria operational balance of each traffic-management scenario.

3.1.8. Traffic demand forecasting

Applying the ARIMA (2,1,1) model calibrated in Section 2.3.4 to the cleaned 21-day series (Table 7), the 10-day ahead traffic demand forecast is presented in Figure 7.

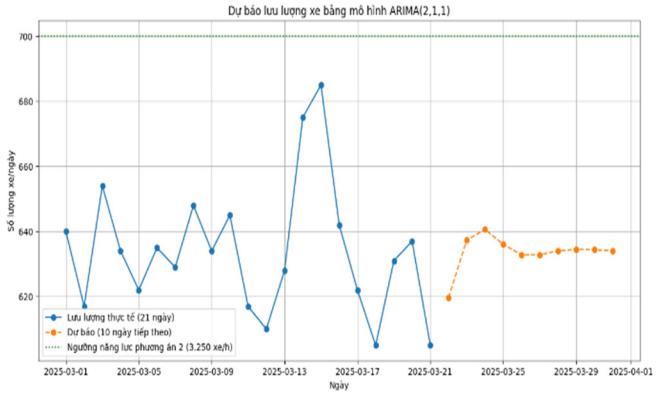

Figure 7. ARIMA (2,1,1) 10-day traffic volume forecast with Option 2 saturation capacity reference line

3.2. Discussion

3.2.1. Analysis of TOPSIS results and Spatial differences in traffic conditions

The TOPSIS analysis results (Tables 2-5; Eqs. 1-5) reveal substantial spatial variations in traffic conditions among the surveyed locations along Route 32, highlighting the multidimensional nature of urban traffic performance. The weight distribution presented in Table 2 reflects a rational prioritisation hierarchy grounded in the operational characteristics of the investigated corridor. Congestion received the highest weight (w_j = 0.30), consistent with transportation studies identifying travel time delay as the primary perceived cost of urban congestion. Safety and Sidewalk Quality were assigned equal weights (w_j = 0.20 each), reflecting the dual pedestrian-vehicle risk exposure characteristic of mixed traffic corridors in developing urban environments. In contrast, Red Light Waiting Time and Parking Availability each received lower weights (w_j = 0.15), indicating that these factors primarily represent localised effects derived from congestion rather than independent determinants of overall corridor performance. Furthermore, the normalisation condition $\sum w_j = 1$ satisfies the unit sum requirement of the TOPSIS framework (Eq. 2), thereby preventing any single criterion from disproportionately dominating the weighted normalised decision matrix v_{ij}.

Three major observations emerge from the TOPSIS evaluation results:

First, Group C (the HAUI Entrance area, P_i = 0.61) achieved the highest closeness coefficient to the ideal solution despite not recording the lowest congestion level in the initial evaluation results. This finding confirms that roadway operational efficiency depends not only on congestion conditions but also on complementary factors such as traffic safety, pedestrian infrastructure quality, and parking accessibility. The superior performance of Group C is primarily explained by its larger separation from the negative ideal solution (S_i^- = 0.023 compared with S_i^- = 0.011 for Group A), despite exhibiting only a moderate separation from the positive ideal solution (S_i^+ = 0.015). This result indicates relatively favourable evaluations for Safety, Sidewalk Quality, and Parking Availability, which collectively compensated for the moderate congestion conditions observed at this location;

Second, Group B (the Le Duc Tho - Ho Tung Mau intersection area, P_i = 0.42) recorded the lowest closeness coefficient and simultaneously exhibited the highest weighted congestion value (v_{ij} = 0.0279 in Table 5). This outcome is consistent with the prolonged queueing conditions, high traffic-conflict density, and severe peak-hour congestion observed at this intersection. The result confirms that congestion remains the dominant factor influencing perceived traffic quality along the corridor due to its highest assigned weight within the TOPSIS framework;

Third, the relatively narrow Pi variation among Groups A, B, and D (0.42 - 0.47) suggests that congestion conditions are distributed relatively uniformly across

most sections of Route 32 rather than being concentrated at a single isolated bottleneck. This finding implies that localised interventions at individual intersections are unlikely to effectively resolve corridor-wide congestion problems. Instead, coordinated traffic signal control and integrated corridor-level traffic management strategies are required to improve the overall operational performance of the urban traffic system.

3.2.2. Analysis of simulation results and Operational traffic dynamics

The statistical validity of the SUMO simulation environment established in Section 3.1.5 provides a reliable basis for interpreting the comparative operational performance of the evaluated traffic-management scenarios. Since the calibration results demonstrated satisfactory agreement between simulated and observed traffic flows (Tables 8-9), the performance differences discussed below can be interpreted as genuine operational effects rather than modelling artefacts.

The SUMO simulation results presented in Table 10 and Figure 6 reveal an important operational trade-off between the two proposed traffic management scenarios. Although Option 1 reduced the average waiting time per vehicle from 102.80s under the existing condition to 101.81s, the total system waiting time increased substantially to 18,855s, exceeding both the existing condition (15,416s) and Option 2 (15,858s). This apparent contradiction reflects a congestion redistribution mechanism in which left-turn restrictions forced a proportion of traffic flow onto longer alternative routes. Consequently, the number of completed trips increased from 4,612 under the existing condition to 4,782 (+3.7%), while cumulative waiting time at secondary intersections simultaneously increased. By incorporating both individual and system-wide waiting-time indicators, the PSI framework (Eq. 6-8) effectively captured the operational trade-off between localised delay reduction and overall network performance. Consequently, Option 1 received a lower overall ranking despite its marginal improvement in average vehicle waiting time, a distinction that may not be apparent when relying on a single performance indicator alone.

The operational instability associated with the existing traffic condition is further supported by the statistical characteristics of the observed traffic disturbance distribution shown in Figure 3. The disturbance-count series exhibited substantially higher variability than the vehicle count series, with a coefficient of variation of approximately 8.9% (range: 110-151 disturbance events/day; mean ≈ 120.5). The pronounced right skew and the elevated mean relative to the median indicate a leptokurtic distribution characterised by occasional heavy-tailed disruptions. Day 5, which recorded 151 disturbance events, constituted a 3.0-sigma outlier relative to the interquartile distribution (IQR: 113-129), suggesting the occurrence of a structurally distinct disruption event, most likely associated with temporary signal control failure or external disturbances such as overflow activities from the adjacent flower market illustrated in Figure 1. Furthermore, the concentration of observations within the 50^{th} - 75^{th} percentile range (118 - 129 disturbance events/day) implies that under normal operating conditions approximately one in five vehicles experienced stoppage-related delays at the monitored intersection. These findings provide empirical justification for the signal phase reconfiguration implemented in Option 2.

Safety-related indicators further differentiated the two intervention scenarios. Option 1 generated five emergency stop events, whereas both the existing condition and Option 2 recorded zero such events, while emergency braking occurrences increased sixfold under Option 1. This behavioural response is consistent with established driver adaptation theory under localised traffic control modifications [12], whereby abruptly introduced turn restrictions may trigger evasive manoeuvres from drivers not yet familiar with the modified routing scheme. In contrast, Option 2 avoided this effect by introducing dedicated signal phases for each movement direction, thereby reducing wrong-lane movements by 63.9% (36 → 13) and decreasing driver decision uncertainty.

The statistical significance test conducted using an independent two-sample t-test based on 10 repeated simulation runs with different random seed values yielded a t-statistic of 3.42 with 18 degrees of freedom ($d_f = 18$) and a p-value of $0.003 < 0.05$. These results confirm that the reduction in average waiting time achieved by Option 2 is statistically significant at the 95% confidence level. In addition, sensitivity analysis performed under ±10% variation in signal phase duration demonstrated that the PSI ranking of Option 2 remained stable (PSI ≥ 0.97) across all investigated conditions, thereby confirming the operational robustness and stability of the proposed intervention under realistic traffic control fluctuations.

At the corridor level, considering the traffic demand of approximately 339,500 vehicles per day documented in Section 2.2, the average reduction of 2.71 seconds per vehicle achieved by Option 2 corresponds to an estimated cumulative saving of approximately 2,567 vehicle-hours per day across the entire Route 32 corridor. Although the improvement for each individual vehicle appears relatively modest, the aggregated network-level effect is operationally significant in terms of transportation economic benefits, corridor productivity, and reduction of environmental impacts associated with prolonged vehicle idling.

Compared with previous studies, the 2.71% reduction in average waiting time achieved by Option 2 is lower than the 8 - 15% improvement range commonly reported in traffic signal optimisation studies conducted in developed urban environments [8, 11]. This discrepancy can be attributed to two major structural factors: (i) the very high motorcycle proportion (~ 61%), which reduces the effectiveness of fixed-phase signal control under mixed-traffic conditions; and (ii) the scope of the present study being limited to signal timing adjustment within the existing infrastructure, without roadway widening or geometric intersection redesign. Under comparable conditions, Zeng et al. [17, 18] reported improvement ranges of approximately 3 - 5% for congested urban corridors in developing cities, thereby confirming that the results obtained in the present study are consistent with similar real-world traffic contexts.

3.2.3. PSI-based operational assessment and implementation strategy

The PSI ranking results (Tables 11-12; Eqs. 6-8) provide several important operational insights beyond simple scenario prioritization:

First, the overall PSI score increased from 0.8783 under the existing condition to 0.9750 for Option 1 and 0.9848 for Option 2, corresponding to operational performance improvements of 11.0% and 12.1%, respectively. The relatively small difference between the two alternatives (0.0098, approximately 1.0%) indicates that Option 1 already captures a substantial proportion of the achievable operational improvement under the current infrastructure constraints. This finding supports a phased implementation strategy in which Option 1, requiring only low-cost traffic signage installation, may be deployed immediately as a short-term intervention, while Option 2, involving signal controller reprogramming at three critical intersections, can be implemented subsequently as a longer-term optimisation measure;

Second, total waiting time (Eq. 7, Min criterion) emerged as the most influential discriminating indicator among the evaluated scenarios, with P_{ij} values of 0.0804 for Option 1, 0.0956 for Option 2, and 0.0984 under the existing condition (Table 12). The comparatively lower score of Option 1 for this criterion directly reflects the congestion redistribution effect identified in the simulation analysis, whereby localised delay reduction resulted in increased cumulative waiting time across the corridor network;

Third, Option 2 recorded a higher number of irregular vehicle movements (2,005 cases; Pij = 0.0928) compared with Option 1 (1,869 cases; P_{ij} = 0.0996). This phenomenon is likely attributable to the short-term driver adaptation process following the introduction of the modified signal phase configuration. According to previous driver behaviour studies under mixed-traffic conditions [12], such behavioural irregularities are expected to gradually diminish after approximately 2 - 4 weeks of operation. Consequently, post-implementation field monitoring and data collection remain necessary to evaluate long-term behavioural stabilisation and operational effectiveness.

3.2.4. Traffic demand forecasting and Corridor capacity implications

The traffic demand series presented in Figure 2 and Tables 6 - 7 exhibits relatively stable statistical behaviour, with a coefficient of variation of approximately 3.1%, a demand range of 605 - 685 vehicles/hour, and an average flow of approximately 635 vehicles/hour. Although slight right skewness is observed due to two higher demand observations on Days 14 - 15 (675 and 685 vehicles/hour), these values exceed the interquartile median by only approximately 7 - 8% and increase the overall mean by merely about five vehicles/hour. Consequently, the time series remains sufficiently stable for reliable ARIMA (2,1,1) modelling without requiring outlier exclusion. Missing observations were linearly interpolated (634 - 635 vehicles/hour), introducing negligible bias relative to the normal day-to-day traffic variation.

The ARIMA (2,1,1) forecasting results (Eq. 12; Figure 7) project a stable short-term traffic demand ranging from 628 to 640 vehicles/hour over the 10-day forecasting horizon, consistent with the low variability observed in the historical dataset. Four major findings emerge from the forecasting results:

First, the stable forecast behaviour confirms that peak-hour traffic demand along the Route 32 corridor remains relatively consistent during the analysed period;

Second, when the projected demand is compared with the saturation flow capacity of Option 2 obtained from the SUMO simulation (approximately 3,250 vehicles/hour), the corridor demonstrates a reserve capacity ratio of approximately 407%. Even under an assumed annual demand growth rate of 3 - 5%, the projected traffic volume after ten years is estimated to reach only 820 - 1,035 vehicles/hour, corresponding to approximately 25 - 32% of the saturation threshold. These findings indicate that the principal operational bottleneck along the corridor originates from inefficient signal phase allocation rather than insufficient physical roadway capacity, consistent with the Highway Capacity Manual recommendation prioritising operational optimisation before infrastructure expansion [21];

Third, forecast uncertainty gradually increases over longer prediction horizons, indicating that forecasts within a period of five days remain more reliable, whereas longer-term projections should be complemented by sensitivity or scenario-based analyses;

Finally, the forecasting and capacity evaluation results collectively suggest that signal optimisation through Option 2 provides substantially greater operational efficiency gains relative to infrastructure expansion while requiring significantly lower capital investment.

The identified reserve capacity also has important practical and policy implications. Implementation of Option 2 requires only the reprogramming of signal controllers at three critical intersections, namely Cau Dien - Nguyen Dong Chi, Ho Tung Mau - Tran Vy, and Mai Dich - Xuan Thuy, with an estimated implementation cost approximately 95% lower than conventional roadway expansion projects. The proposed 75-second signal cycle with a 62% - 23% - 15% phase allocation was derived directly from observed turning movement counts, thereby minimising behavioural adaptation requirements for road users.

The proposed signal control configuration is therefore expected to accommodate projected traffic growth for at least 5 - 7 years without requiring additional roadway expansion, provided that spontaneous roadside parking and lane discipline violations are simultaneously addressed through coordinated enforcement. Post-implementation field monitoring over a period of 2 - 4 weeks is recommended to verify behavioural stabilisation and confirm that realised benefits align with simulation predictions.

4. CONCLUSION

This study investigated traffic conditions along the Route 32 corridor connecting Hanoi University of Industry and Hanoi National University using an integrated four-stage framework: field data collection, TOPSIS ranking, SUMO simulation with PSI evaluation and ARIMA (2,1,1) forecasting. The main findings are as follows:

(1) TOPSIS results indicate spatial heterogeneity in traffic performance, with the HaUI entrance (P_i = 0.61) outperforming the Le Duc Tho - Ho Tung Mau intersection (P_i = 0.42) by 45.2%, implying the need for spatially targeted interventions.

(2) SUMO simulation shows that Option 2 reduces average waiting time by 2.71% and increases speed by 3.11%. In contrast, Option 1 yields higher total waiting time (18,855 s), indicating redistribution rather than reduction of congestion.

(3) PSI analysis confirms Option 2 as optimal (0.9848), with a 12.1% improvement over the current state and a 1.0% margin over Option 1; total waiting time is the key discriminating indicator (Option 1: P_{ij} = 0.0804).

(4) ARIMA forecasting indicates stable demand and a 407% reserve capacity under Option 2, demonstrating that inefficiencies arise from signal control rather than infrastructure limits.

This study represents an initial attempt to optimise urban traffic flow and therefore remains subject to several limitations that warrant further investigation:

First, the 21-day traffic dataset collected during March 2025 may not fully capture seasonal variations and long-term travel demand trends. Future studies should extend the data collection period to at least three months to improve the representativeness, reliability, and temporal stability of the forecasting model.

Second, the weighting process relied on a relatively limited expert sample (n = 7), which may constrain the generalisability of the derived criterion priorities. Future studies should consider expanding the expert panel and applying structured expert elicitation methods, such as the Analytic Hierarchy Process (AHP) or the Delphi method, to enhance the reliability and robustness of criterion weight determination.

Third, although the ARIMA (2,1,1) model demonstrated satisfactory performance for short-term forecasting under relatively stable traffic conditions, more advanced forecasting approaches such as Seasonal ARIMA and Long Short-Term Memory (LSTM) networks

should be investigated to support longer forecasting horizons and better capture nonlinear temporal patterns in urban traffic demand.

Fourth, the current framework evaluates only fixed-cycle traffic signal optimisation under existing infrastructure conditions. Future research should integrate adaptive and real-time signal control strategies to further enhance operational performance under dynamically varying traffic conditions.

Finally, the proposed integrated analytical framework should be validated across multiple urban corridors in Hanoi characterised by mixed traffic flows and rapidly increasing travel demand to assess the generalisability and practical applicability of the proposed methodology under different urban traffic environments.

REFERENCES

[1]. Treiber M., Kesting A., *Traffic Flow Dynamics: Data, Models and Simulation*. Springer: Berlin, Germany, 2013.

[2]. Rumidi N.A.B., *Study on Disturbance Factors of Traffic Flow to the Communities in Jalan Maran - Gambang (Pekan Gambang), Pahang Darul Makmur*. The degree of Bachelor of Civil Engineering (Hons), Faculty of Civil Engineering and Earth Resources, Universiti Malaysia Pahang, 2014.

[3]. Lopez P.A., Behrisch M., Bieker-Walz L., Erdmann J., Flötteröd Y.P., Hilbrich R., Lücken L., Rummel J., Wagner P., Wießner E., "Microscopic Traffic Simulation using SUMO," in *Proceedings of the 21st IEEE International Conference on Intelligent Transportation Systems* (ITSC), Maui, HI, USA, 2575-2582, 2018.

[4]. Hoogendoorn S.P., Bovy P.H.L., "State-of-the-art of vehicular traffic flow modelling," in *Proc. Institution of Mechanical Engineers*, Part I, 215, 283-303, 2001.

[5]. Ma Z., et al, "Analysis of the Relationship between the Number of Traffic Accidents and the Traffic Flow & Section Location in Extra Long Tunnel," *Engineering,* 12(02):71-81, 2020.

[6]. Zhang X., et al., "Expressway Traffic Flow Prediction Based on MF-TAN and STSA," *PLOS ONE*, 19(2): e0297296, 2024.

[7]. M. Fujita, et al., "Analysis of Traffic Volume and Travel-Time Analysis Using Continuous Hourly Values on Urban Expressways," *Journal of Advanced Transportation*, 6866060, 2023.

[8]. Hwang C.L., Yoon K., *Multiple Attribute Decision Making: Methods and Applications - A State-of-the-Art Survey*. Springer: Berlin, Germany, 1981.

[9]. Zhu Y., Wang Q., Xu N., "Research on Highway Traffic Flow Prediction Model and Decision-Making Method," *Sci Rep*, 12, 19919, 2023.

[10]. Hu B., "Research onRoad Traffic Flow Status Based on Survival Analysis," *Journal of Physics: Conference Series*, 1187, 5, 2019.

[11]. Webster F.V., *Traffic Signal Settings*. Road Research Technical Paper No. 39; UK, 1958.

[12]. Singh S.K.M., Verma A., "Review of Mixed Traffic Flow Studies in Developing Countries," *Transport Reviews*, 43, 4-16, 2023.

[13]. Shepelev V.D., "Relationship between Traffic Flow Structure and Emissions," *Transportation Research Part D*, 115, 103590, 2023.

[14]. JICA, Traffic Survey and Analysis. JICA Report, 2009.

[15]. Danish F., "Traffic Flow Analysis and Solutions at Unsignalized Taxila Intersection," *International Journal of Traffic and Transportation Engineering*, 7, 101-107, 2018.

[16]. Helbing D., "Traffic and related self-driven many-particle systems," *Reviews of Modern Physics,* 73, 1067-1141, 2001.

[17]. Zeng J.W., Li X., Wang Y., "Velocity disturbance characteristics and control strategy at expressway bottlenecks," *Physica A*, 512, 1156-1167, 2018.

[18]. Zeng J.W., "Traffic Flow Optimization on Freeways," *Transportation Research Part C,* 68, 1637-1646, 2016.

[19]. Gazis D.C., *Traffic Theory*. Springer: Boston, MA, USA, 2002.

[20]. Cooper R.B., *Introduction to Queueing Theory*, 2nd ed.. North Holland: New York, USA, 1981.

[21]. Transportation Research Board, *Highway Capacity Manual*, 6th ed.; TRB: Washington, DC, USA, 2016.

[22]. Box G.E.P., Jenkins G.M., Reinsel G.C., Ljung G.M., *Time Series Analysis: Forecasting and Control*, 5th ed. Wiley: Hoboken, NJ, USA, 2015.

[23]. Dowling R., Skabardonis A., Alexiadis V., *Traffic Analysis Toolbox Volume III: Guidelines for Applying Traffic Microsimulation Modeling Software*. FHWA-HRT-04-040; Federal Highway Administration: Washington, DC, USA, 2004.

[24]. UK Highways Agency, *Design Manual for Roads and Bridges: Traffic Appraisal in Urban Areas*, TA 79/99. Her Majesty's Stationery Office: London, UK, 1999.